Theoretical and Experimental Investigation of the Compressible Free Mixing of Two Dissimilar Gases

COLEMAN DUP. DONALDSON* AND K. EVAN GRAY†
Aeronautical Research Associates of Princeton Inc., Princeton, N. J.

An extension and improvement of Warren's momentum integral method for predicting the turbulent mixing and decay of axially symmetric, compressible, free jets to the case of the mixing of dissimilar gases is discussed. Two ideal gases having different molecular weights and specific heats are treated with the assumption that the local turbulent mixing rate at each axial location depends upon a suitably chosen local reference Mach number. This method of analysis is then compared with the results of a series of jet-mixing experiments carried out on helium, methane, nitrogen, carbon dioxide, and freon jets mixing in air. Mach numbers ranging from 0.75 to 3.30 were investigated. The character and mixing rates of both properly and improperly expanded supersonic jets were studied. It is concluded from a comparison of these data with the theoretical method presented that a general relationship exists, at each axial position in the jet, between a local mixing rate parameter and the local Mach number. This general relationship is independent, within the accuracy of these experiments, of the physical properties or the thermodynamic state of the mixing gases.

1. Introduction

THERE has been much interest recently in the turbulent mixing rates of high-temperature free jets and wakes. A great deal of this interest has been generated by the problem of predicting the thermodynamic and electrical properties of decaying rocket exhaust plumes and wakes of re-entry vehicles. There are, in addition to these two primarily military problems, a great number of instances throughout our present technology where the turbulent mixing characteristics of free jets and wakes are of considerable importance.

There are essentially three methods in use today by which the decay of free jets and wakes are studied. These consist of two methods that have been in use for some time, and a method that has become available within the last few years as a result of the rapid development and use of high-speed computers. The three methods are: 1) the simple momentum integral method, 2) solution of the equations of motion when certain assumptions are made which render these equations tractable to existing analytical techniques, and 3) step-by-step numerical solution of the equations on high-speed digital computers.

All of these methods depend ultimately on experimental turbulent mixing data since an essential part of all these techniques is the specification of the local eddy viscosity of the particular turbulent flow in question at, at least, one general location in the mixing region; and this is a task quite beyond the power of existing theory.

An excellent bibliography of both experimental and theoretical work on turbulent mixing prior to 1950 is given in a paper by Forstall and Shapiro.[1] Excellent reviews of more recent work on turbulent mixing may be found in papers by Libby,[2] Ferri, Libby, and Zakkay,[3] and Ferri.[4] Without attempting to review the literature further at this time, two papers from among this more recent work should be mentioned specifically. The first, by Warren,[5] presents the results of a number of experiments on the mixing of properly expanded, heated jets into quiescent air. In these experiments, the initial Mach number of the air in the jets studied was varied between approximately 0.7 and 2.6. These experimental results were analyzed by means of the momentum integral technique and the general character or mixing rate of the jets studied presented in terms of a mixing-rate parameter that was a function of Mach number. It is typical of the analysis or description of mixing phenomena by means of the momentum integral technique that only general trends of characteristics of the motions involved can be described.

The second paper that should be mentioned is one by Libby.[2] In this paper, an attempt is made to go beyond the momentum integral technique and look for more complete information concerning the nature of jet mixing by means of analytical solutions of approximate equations of motion. The method presented by Libby was developed in connection with the mixing of two coaxial streams of dissimilar gases, the outer being of infinite extent. This paper is important because the analysis developed forms the basis for much subsequent research on turbulent mixing (see, for example, Refs. 3, 4, 6, and 7).

In conjunction with some recent work at Aeronautical Research Associates of Princeton (ARAP), a number of simple mixing experiments were carried out. In these tests, the decay and spread of both properly and improperly expanded free jets of several gases in an ambient atmosphere of air were measured. These measurements were analyzed by developing an extension of Warren's method[5] for predicting free-jet decay and comparing the experimental results with theoretical calculations. Since the results of these experiments are thought to be of interest, these experiments and their analysis are presented here in the form of a mixing-rate parameter that is apparently, to first order, only a function of a suitably chosen local Mach number.

2. Analysis

In the discussion that follows, we will assume a free mixing to take place between an initially irrotational and axially symmetric stream of an ideal gas distinguished by the subscript 1 and another ambient gas (subscript 2) that also is ideal. These two gases are, for the purpose of predicting the basic mixing process, assumed to be inert chemically. Under these circumstances, the density of the gas in any region of interest is given by the expression

$$\rho = \rho_1 + \rho_2 = \rho(c_1 + c_2) \tag{2.1}$$

where c_1 and c_2 are the mass fractions of gases 1 and 2, respec-

Presented as Preprint 65-822 at the AIAA Aerothermochemistry of Turbulent Flows Conference, San Diego, Calif., December 13–15, 1965; submitted June 20, 1966; revision received August 8, 1966.

* President and Senior Consultant. Associate Fellow AIAA.
† Associate Consultant. Member AIAA.

Reprinted from AIAA JOURNAL

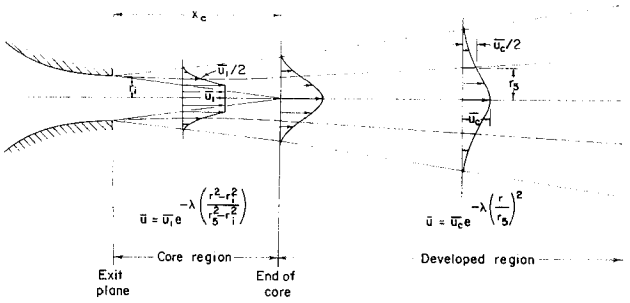

Fig. 1 Idealized jet structure.

tively. The local enthalpy per unit mass is given by

$$h = c_1h_1 + c_2h_2 = (c_1c_{p_1} + c_2c_{p_2})T = \hat{c}_pT \qquad (2.2)$$

where c_{p_1} and c_{p_2} are the constant specific heats at constant pressure of gases 1 and 2. In addition, we will assume that the Prandtl and Schmidt numbers of the two gases and any mixtures thereof are one, and that the Mach number of the turbulence itself in the mixing processes under consideration is small, i.e.,

$$\overline{M_i'^2} = \overline{u_i'^2}/\bar{a}^2 \ll 1$$

Under these circumstances, we can make the customary assumption that the usual Crocco integral

$$\bar{h} + (\bar{u}^2/2) = A\bar{u} + B \qquad (2.3)$$

and the associated concentration integrals

$$\bar{c}_\alpha + a_\alpha\bar{u} = b \qquad (2.4)$$

hold throughout the mixing region. In the preceding equations we have followed the usual practice of denoting mean quantities by a superscript bar and all fluctuations from these mean values by means of a prime.

The equations we shall need under the foregoing assumptions to describe the mixing region are then

$$(\partial/\partial x)(\bar{\rho}\bar{u}r) + (\partial/\partial r)(\bar{\rho}\bar{v}r + \overline{\rho'v'r}) = 0 \qquad (2.5)$$

$$\bar{\rho}\bar{u}r(\partial\bar{u}/\partial x) + (\bar{\rho}\bar{v} + \overline{\rho'v'})r(\partial\bar{u}/\partial r) = -(\partial/\partial r)(\bar{\rho}\overline{u'v'}) \qquad (2.6)$$

$$\partial\bar{p}/\partial r = -(\partial/\partial r)(\bar{\rho}\overline{v'^2}) + (\bar{\rho}\overline{w'^2} - \bar{\rho}\overline{v'^2}/r) \qquad (2.7)$$

$$\bar{w} = 0 \qquad (2.8)$$

together with the condition that mean quantities are independent of ϕ. In these equations, p is the pressure, and a cylindrical coordinate system (r, ϕ, x) with velocity components (v, w, u) is used. In addition to the assumptions given previously, which permitted the neglect of terms of the form $\overline{\rho'u'}$, we have also neglected a term in Eq. (2.6) of the form $\partial(\bar{\rho}\overline{u'^2} - \bar{\rho}\overline{v'^2})/\partial x$. If we eliminate $\bar{\rho}\bar{v} + \overline{\rho'v'}$ from Eq. (2.6) by means of Eq. (2.5), we obtain

$$r\bar{\rho}\bar{u}\frac{\partial\bar{u}}{\partial x} - \frac{\partial\bar{u}}{\partial r}\int_0^r \frac{\partial}{\partial x}(r\bar{\rho}\bar{u})dr = -\frac{\partial}{\partial r}(r\overline{\rho u'v'}) = \frac{\partial}{\partial r}(r\tau) \qquad (2.9)$$

With the results just presented in hand, we are able to discuss the extension of Warren's method for predicting the decay of axially symmetric free jets to the case of the mixing of two separate and chemically inert gases. Since Warren's method is a momentum integral method, we integrate Eq. (2.9) with respect to r from the axis of symmetry to some particular radius $r = r_*$. The result is

$$\frac{d}{dx}\int_0^{r_*} \bar{\rho}\bar{u}^2rdr = \bar{u}_*\frac{d}{dx}\int_0^{r_*}\bar{\rho}\bar{u}rdr + \tau_*r_* \qquad (2.10)$$

This equation states that the net rate of change with respect to axial distance of the momentum in the jet out to an arbitrary radius r_* is equal to the change in momentum resulting from mass addition with velocity $\bar{u}_*$ at radius r_* plus the change in momentum resulting from the shear taking place at radius r_*. Since r_* is arbitrary, we are free to choose any radius we wish and thus pick the customary one, namely the radius at which the local velocity has fallen to exactly one-half the value of the velocity on the centerline for the same axial location, which we designate r_5. If, on the other hand, we pick a very large radius, the two terms on the right-hand side of Eq. (2.10) vanish, since $\bar{u}_* \to 0$ and $\tau_* \to 0$ as $r_* \to \infty$. Therefore, the net change of the total momentum flux passing through each plane normal to the axis of the jet is zero. Thus, we have produced two equations out of expression (2.10). One is expression (2.11) with r_5 and τ_5 substituted for r_* and τ_*, and the other is an expression for the fact that the total axial momentum flux is invariant. Thus,

$$\frac{d}{dx}\int_0^{r_5} \bar{\rho}\bar{u}^2rdr = \bar{u}_5\frac{d}{dx}\int_0^{r_5}\bar{\rho}\bar{u}rdr - \tau_5r_5 \qquad (2.11)$$

$$\int_0^\infty \bar{\rho}\bar{u}^2rdr = \text{const} = \frac{\bar{\rho}_1\bar{u}_1^2r_1^2}{2} \qquad (2.12)$$

Velocity Profiles

A relationship between $\bar{u}$ and r can be obtained by assuming some velocity profile across the jet. Here we can lean upon experimental evidence that shows that the general character of free jets can be approximated quite well by the idealized jet structure illustrated in Fig. 1. It is seen that the jet can be considered as being made up of two distinct regions. Close to the jet exit there is a region in which a "core" of fluid, moving at the exit velocity of the jet, is embedded. This core diminishes in width in a downstream direction to a point at which it ceases to exist. The distance from the exit plane to this point is known as the core length and defines the extent of this first or core region. Outside the core, turbulent mixing is taking place and, as can be seen from Fig. 1, this mixing grows laterally as the width of the core diminishes.

Downstream of the core region, the velocity profiles become similar in shape, changing only in scale. Here, with increasing distance downstream, the velocity on the centerline decreases whereas the width of the jet continues to increase. It has been shown by several workers[8,9] that for the incompressible, single-gas, turbulent free jet, the centerline velocity in this second or "developed" region is proportional to $1/x$ whereas the spreading of the jet is proportional to x.

From the preceding observations, it is clear that two velocity profiles are needed, one for the core region and one for the developed region. The profiles used by Warren[5] appear to be the most useful. These profiles are

Core region

$$\bar{u} = \bar{u}_1e^{-\lambda(r^2-r_i^2/r_5^2-r_i^2)} \qquad r \geq r_i$$
$$= \bar{u}_1 \qquad r \leq r_i \qquad (2.13)$$

Developed region

$$\bar{u} = \bar{u}_ce^{-\lambda[(r/r_5)]^2} \qquad (2.14)$$

Here, r_i refers to the radius to the outer edge of the core and r_5 to the radius at which the local velocity $\bar{u}$ is one-half of the centerline value $\bar{u}_c$. Note that r_5 is a convenient measure of the spread of the jet, representing as it does the "half velocity" point for a particular station. It can easily be shown that with the foregoing definition of r_5, $\lambda = \ln 2$.

Turbulent Shear Stress

We turn now to an evaluation of the turbulent shear stress. We will assume, following Warren, that the local value of this stress is given by

$$\tau = -\rho\overline{u'v'} = K\rho b U_s(\partial\bar{u}/\partial r) \tag{2.15}$$

where K is the mixing-rate factor, b is a typical local scale length, ρ is the local density, and U_s is a typical local velocity difference. For the core region of the jet (again following Warren), we choose b equal to $r_5 - r_i$ and U_s equal to $\bar{u}_1/2$, and in the developed region we take b equal to r_5 and U_s equal to $\bar{u}_c/2$. Thus, we have for the core region,

$$\tau = K\rho(r_5 - r_i)(\bar{u}_1/2)(\partial\bar{u}/\partial r) \tag{2.16}$$

and for the developed region,

$$\tau = K\rho r_5(\bar{u}_c/2)(\partial\bar{u}/\partial r) \tag{2.17}$$

Local Enthalpy

The equation for the local enthalpy [Eq. (2.3)] can, by utilizing the boundary conditions $\bar{h} = h_\infty$ when $\bar{u} = 0$ and $\bar{h} = h_1$ when $\bar{u} = \bar{u}_1$, be written

$$\bar{h} = h_\infty + (h_1^0 - h_\infty)(\bar{u}/\bar{u}_1) - (\bar{u}_1^2/2)(\bar{u}/\bar{u}_1)^2 \tag{2.18}$$

where

$$h_1^0 = h_1 + \bar{u}_1^2/2$$

Local Mass Fractions

In the case of the mixing of a rocket exhaust with the air surrounding it, there exist two $\bar{c}_\alpha$; $\bar{c}_r$, the local mass fraction of the exhaust gas and $\bar{c}_a$, the local mass fraction of the surrounding gas. From Eq. (2.4), utilizing the boundary conditions $\bar{c}_r = 0$ when $\bar{u} = 0$ and $\bar{c}_r = 1$ when $\bar{u} = \bar{u}_1$, one obtains

$$\bar{c}_r = \bar{u}/\bar{u}_1 \tag{2.19}$$

Since the boundary conditions on $\bar{c}_a$ are $\bar{c}_a = 1$ when $\bar{u} = 0$ and $\bar{c}_a = 0$ when $\bar{u} = \bar{u}_1$, we find that

$$\bar{c}_a = 1 - (\bar{u}/\bar{u}_1) \tag{2.20}$$

Other Local Properties

In order to solve Eqs. (2.11) and (2.12) for the spread and decay of a given jet, we shall have to have an expression for the local mean density in terms of the local pressure $\bar{p}$, the local enthalpy $\bar{h}$, and the concentrations $\bar{c}_a$ and $\bar{c}_r$. This can be accomplished by means of the perfect gas law

$$p = \rho(\mathfrak{R}/m)T \tag{2.21}$$

where $\mathfrak{R}$ is the universal gas constant and m is the local molecular weight of the gas mixture. In what follows, since we will be using expressions for $\bar{h}$, $\bar{c}_a$, and $\bar{c}_r$ that are known to be only approximately true, we will neglect certain correlations that appear in the exact expression for $\bar{\rho}$ from Eq. (2.21) and write simply

$$\bar{\rho} = (\bar{m}\bar{p}/\mathfrak{R}\bar{T}) = (\bar{m}\bar{c}_p\bar{p}/\mathfrak{R}\bar{h}) \tag{2.22}$$

Consistent with the approximation inherent in using Eq. (2.22), we may simplify matters exceedingly if, instead of using the exact expression for $\bar{p}$ given by Eq. (2.7), we assume the $\bar{\rho}$ is everywhere equal to the ambient pressure p_∞. The local density can then be written

$$\bar{\rho} = \frac{p_\infty\left[(c_{p_1} - c_{p_\infty})\left(\frac{\bar{u}}{\bar{u}_1}\right) + c_{p_\infty}\right]}{\mathfrak{R}\left[\left(\frac{1}{m_1} - \frac{1}{m_\infty}\right)\left(\frac{\bar{u}}{\bar{u}_1}\right) + \frac{1}{m_\infty}\right]\left[h_\infty + (h_1^0 - h_\infty)\left(\frac{\bar{u}}{\bar{u}_1}\right) - \left(\frac{\bar{u}_1^2}{2}\right)\left(\frac{\bar{u}}{\bar{u}_1}\right)^2\right]} \tag{2.23}$$

It may be useful to set forth the expressions for several other local mean quantities within the approximations mentioned previously. Thus,

$$\bar{c}_p = (c_{p_1} + c_{p_\infty})(\bar{u}/\bar{u}_1) + c_{p_\infty} \tag{2.24}$$

$$\bar{m} = [(1/m_1 - 1/m_\infty)(\bar{u}/\bar{u}_1) + (1/m_\infty)]^{-1} \tag{2.25}$$

$$\gamma = [1 - (\mathfrak{R}/\bar{m}\bar{c}_p)]^{-1} \tag{2.26}$$

$$M = \{[\bar{u}_1^2/(\gamma - 1)\bar{h}](\bar{u}/\bar{u}_1)^2\}^{1/2} \tag{2.27}$$

Spreading and Decay

Reviewing the progress to this point, we find that we have two basic equations that describe the flow, Eqs. (2.11) and (2.12). In addition, we have developed expressions for‡ 1) ρ in terms of u [Eq. (2.23)]; 2) u in terms of r, r_5, and r_i for the core [Eq. (2.13)], and u in terms of r, r_5, and u_c for the developed region [Eq. (2.14)]; 3) τ in terms of K, r_5, and r_i for the core [Eq. (2.16)], and τ in terms of K, r_5, and u_c for the developed region [Eq. (2.17)]. When these expressions are substituted into the two flow equations, we will find that there remain the three unknowns: K, r_5, and r_i when the two equations are written for the core region; and K, r_5, and u_c when the same equations are written for the developed region.

Therefore, if K can be determined empirically from experimental test data, then there remain just two unknowns (r_5 and r_i in the core, and r_5 and u_c in the developed region) and two equations applicable to each region. These remaining quantities can be found, thereby providing the solution to the decay and spreading behavior of the jet. The local velocity anywhere in the flow can then be obtained by use of $r_5(x)$, $r_i(x)$, and $u_c(x)$ and the velocity profile equations (2.13) and (2.14).

The key to the success of the present method of analysis is, therefore, the satisfactory determination of the shear stress parameter K. In the work of Warren, K is assumed a constant throughout the flow for a particular jet. Warren correlated K with the initial jet Mach number only, finding that K was dependent primarily on the initial Mach number, but not on the initial enthalpy. Specifically, he suggested the relation

$$K = 0.0434 - 0.0069\,M_1$$

In the present study we attempt to show that K is primarily dependent on only a suitably chosen local Mach number and not on enthalpy ratio or molecular weight ratio, both factors having been properly taken into account through the density factor in the equation for τ. One possible choice of local Mach number is the local Mach number on the jet centerline. However, the maximum shear at a given axial station does not occur at the centerline but at some finite radius where the product of ρ and $\partial u/\partial r$ is a maximum. This particular radius is, in general, not too far removed from the half-velocity radius r_5. This latter quantity is already slated for evaluation, and the velocity (upon which all the flow parameters including the local Mach number depend) associated with r_5 is by definition simply $u_c/2$. Therefore, the local conditions at r_5 appear to be a judicial choice upon which to base a study of the parameter K, since significant shearing does take place at r_5 and the conditions there are quite readily computed. In what follows, we shall assume K to vary with x and shall seek to correlate K with the local Mach number at the one-half velocity radius, written hereafter as M_5.

‡ In what follows, since there is no chance for confusion, we will drop the superscript bar with the understanding that all quantities are average values.

It is interesting to note that in the core region the centerline velocity is everywhere u_1 and thus the velocity at r_5 is everywhere $u_1/2$. This in turn means that all other flow parameters (including M_5), being functions of u, are also constant at r_5. Thus K, despite our assumption of its dependence on M_5, will be a constant in the core region. In the developed region, on the other hand, the velocity at r_5 is $u_c/2$ where u_c, of course, does vary with x, thereby requiring the other local flow properties at r_5, including M_5 and thus K, also to vary with x. We shall discuss further the evaluation of K in Sec. 3.

To carry out the procedure described in the foregoing for the solution of r_5, r_i, and u_c is an involved process, particularly when performing the integrations and subsequent differentiations indicated in Eqs. (2.11) and (2.12). To prevent becoming entangled in algebraic details, the solution of the jet decay and spreading to be developed below will be in outline form only. The expressions for the several functions that evolve are provided in the Appendix, however, for the convenience of those who may wish to compute numerically a turbulent free jet by this method. Also, only the developed region will be treated here, since the core region solution follows along the same lines with but slightly different expressions for u and τ, as already seen. The derivation for the core is given in the Appendix also.

The first step in our outline of the solution is to nondimensionalize the flow equations (2.11) and (2.12) and the expressions for u, Eq. (2.14), and τ, Eq. (2.17). Using the convention that capital letters represent the suitably nondimensionalized counterparts of the small letter quantities (i.e., $R = r/r_1$, $U = u/u_1$, $X = x/r_1$, etc.), these expressions become

$$\frac{d}{dX}\int_0^{R_5}\left(\frac{\rho}{\rho_\infty}\right)U^2RdR - \frac{U_c}{2}\frac{d}{dX}\int_0^{R_5}\left(\frac{\rho}{\rho_\infty}\right)URdR = \left(\frac{\tau_5}{\rho_\infty u_1^2}\right)R_5 \quad (2.28)$$

$$\int_0^{\infty}\left(\frac{\rho}{\rho_\infty}\right)U^2RdR = \frac{1}{2}\left(\frac{\rho_1}{\rho_\infty}\right) \quad (2.29)$$

where

$$(\tau_5/\rho_\infty u_1^2) = (\rho_5/\rho_\infty)\tfrac{1}{2}KR_5U_c(\partial U/\partial R)_{R_5} \quad (2.30)$$

$$U = U_c e^{-\lambda(R/R_5)^2} \quad (2.31)$$

$$(\rho/\rho_\infty) = [(\mathcal{P}U + 1)/(\mathfrak{M}U + 1)(1 + AU - BU^2)] \quad (2.32)$$

$$\mathcal{P} = (c_{p_1}/c_{p_\infty}) - 1 \quad \mathfrak{M} = (m_\infty/m_1) - 1$$

$$A = (h_1^0/h_\infty) - 1 \quad B = \tfrac{1}{2}(u_1^2/h_\infty)$$

From Eq. (2.31) it can be shown that

$$(\partial U/\partial R)_{R_5} = -(\lambda U_c/R_5) \quad (2.33)$$

and

$$RdR = -(R_5^2dU/2\lambda U) \quad (2.34)$$

Expressions (2.30–2.34) can be substituted into the two flow equations, (2.28) and (2.29). [For the sake of compactness, the density ratio is carried along as ρ/ρ_∞, remembering that it is a known function of U as given by Eq. (2.32).] These substitutions and the necessary change in the limits of integration yield

$$\frac{d}{dX}\left[R_5^2\int_{U_5}^{U_c}\left(\frac{\rho}{\rho_\infty}\right)UdU\right] - \frac{U_c}{2}\frac{d}{dX}\times\left[R_5^2\int_{U_5}^{U_c}\left(\frac{\rho}{\rho_\infty}\right)dU\right] = -\lambda^2KR_5U_c^2\left(\frac{\rho_5}{\rho_\infty}\right) \quad (2.35)$$

and

$$\int_0^{U_c}\left(\frac{\rho}{\rho_\infty}\right)UdU = \frac{\lambda}{R_5^2}\left(\frac{\rho_1}{\rho_\infty}\right) \quad (2.36)$$

Differentiating by parts as indicated, Eq. (2.35) can be rewritten as

$$R_5^2\frac{d}{dX}\int_{U_5}^{U_c}\left(\frac{\rho}{\rho_\infty}\right)UdU - \frac{U_c}{2}R_5^2\frac{d}{dX}\int_{U_5}^{U_c}\left(\frac{\rho}{\rho_\infty}\right)dU + \int_{U_5}^{U_c}\left(\frac{\rho}{\rho_\infty}\right)UdU\frac{dR_5^2}{dX} - \frac{U_c}{2}\int_{U_5}^{U_c}\left(\frac{\rho}{\rho_\infty}\right)dU\frac{dR_5^2}{dX} = -\lambda^2KR_5U_c^2\left(\frac{\rho_5}{\rho_\infty}\right) \quad (2.37)$$

Among the operations indicated previously are five associated with integration. It is possible to obtain closed form expressions for these operations with the aid of Eq. (2.32) for ρ/ρ_∞. It is convenient to represent the five integrals by the following notation:

$$\int_{U_5}^{U_c}\left(\frac{\rho}{\rho_\infty}\right)UdU = I_c - I_5 \quad (2.38)$$

$$\int_{U_5}^{U_c}\left(\frac{\rho}{\rho_\infty}\right)dU = J_c - J_5 \quad (2.39)$$

$$\frac{d}{dX}\int_{U_5}^{U_c}\left(\frac{\rho}{\rho_\infty}\right)UdU = F_c\frac{dU_c}{dX} - F_5\frac{dU_5}{dX} \quad (2.40)$$

$$\frac{d}{dX}\int_{U_5}^{U_c}\left(\frac{\rho}{\rho_\infty}\right)dU = G_c\frac{dU_c}{dX} - G_5\frac{dU_5}{dX} \quad (2.41)$$

$$\int_0^{U_c}\left(\frac{\rho}{\rho_\infty}\right)UdU = I_c - I_0 \quad (2.42)$$

where F, G, I, and J are functions of U given in Appendix B.

Utilizing these expressions in Eqs. (2.36) and (2.37) and realizing that $U_5 = \frac{1}{2}U_c$, we then have

$$I_c - I_0 = \frac{\lambda(\rho_1/\rho_\infty)}{R_5^2} \quad (2.43)$$

$$\left[\frac{U_c}{2}\left(G_c - \frac{1}{2}G_5\right) - \left(F_c - \frac{1}{2}F_5\right)\right]R_5^2\frac{dU_c}{dX} + \left[\frac{U_c}{2}\times(J_c - J_5) - (I_c - I_5)\right]\frac{dR_5^2}{dU_c}\frac{dU_c}{dX} = \lambda^2KR_rU_c^2\left(\frac{\rho_5}{\rho_\infty}\right) \quad (2.44)$$

Equation (2.43) immediately provides R_5 as a function of U_c through I_c

$$R_5 = [\lambda(\rho_1/\rho_\infty)/(I_c - I_0)]^{1/2} \quad (2.45)$$

and hence also

$$\frac{dR_5^2}{dU_c} = -\frac{\lambda(\rho_1/\rho_\infty)}{(I_c - I_0)^2}\frac{dI_c}{dU_c} = -\frac{R_5^2F_c}{(I_c - I_0)} \quad (2.46)$$

for use in Eq. (2.44). Substituting Eqs. (2.45) and (2.46) into (2.44), we obtain

$$f(U_c)(dU_c/dx) = K \quad (2.47)$$

where into $f(U_c)$ are lumped all of the constants and functions of U_c that are then present. This function is given in Appendix B also.

Finally, if Eq. (2.47) is integrated from the start of the developed region X_c to any downstream station, X_*, we have

$$\int_1^{U_{c*}} f(U_c)dU_c = \int_{X_c}^{X_*} KdX \quad (2.48)$$

where U_{c*} is the centerline velocity (nondimensionalized) at X_*. Note that K cannot be brought outside the right-hand integral because of its dependence upon M_5 and hence, in the developed region, upon X. The integral on the left-hand side cannot be obtained in closed form for the general two-gas case (or, for that matter, even for the reduced one-gas case) because of the complex nature of $f(U_c)$. Thus both

integrals must be obtained by numerical integration, a procedure quite feasible, however, on even a modest-sized digital computer.

Fortunately, the lower limit on the right-hand integral X_c can be found in closed form from the analysis for the core region. Briefly, we see from Appendix A that the equation that corresponds to (2.48) for the core region is

$$\int_1^{R_{i*}} f(R_i)dR_i = \int_0^{X_*} K_c dX \qquad (2.49)$$

For this case, however, K_c is a constant throughout the core, as has already been discussed, and thus it can be brought outside the integral. Furthermore, $f(R_i)$ unlike $f(U_c)$ can be integrated in closed form. Therefore, it is possible to write (2.49) as

$$F(R_{i*}) - F(1) = K_c X_* \qquad (2.50)$$

where F represents this closed-form integral. Since we know that R_i goes to zero at the end of the core, we can solve for X_c by substituting X_c for X_* and O for R_{i*} in the preceding expression. Hence,

$$X_c = [F(0) - F(1)/K_c] \qquad (2.51)$$

Thus, with Eqs. (2.45, 2.48, and 2.51) we have solutions for the spreading $R_5(X)$ and the decay $U_c(X)$ in the developed region. (The corresponding equations for the spreading $R_5(x)$ and the decay $R_i(x)$ in the core are available in the Appendix A.)

This now allows us to compute the local velocity anywhere in the flow by means of the velocity profile equations that are written in terms of U_c, R_5, and R_i. Finally, with a knowledge of U, all the other flow parameters of interest can be obtained from the expressions previously given.

3. Comparison of Theory with Experiment—Evaluation of K

We turn to the evaluation of the dependence of the shear stress parameter K on M_5 and the determination of the accuracy with which the behavior of turbulent free jets can be predicted by this method. To accomplish these tasks, two programs were initiated.

First, the equations of the present analysis were coded for solution on a high-speed digital computer. This was done in such a manner that either given K as a function of M_5, the flowfield could be computed, or given the flowfield from experimental results, the dependence of K on M_5 could be obtained. Thus, initially, the evaluation of K could be established from available experimental data and then later, the decay of a jet with any initial conditions could be found by using these values of K.

Second, a series of turbulent jet mixing experiments were performed. These were designed to provide data over a range of values of the initial jet conditions such as molecular weight, enthalpy, Mach number, and jet nozzle over- and under-expansion. The results of these experiments, together with data available in the literature, were then utilized, first to evaluate K and then to compute a complete description of the behavior of velocity decay.

Experimental Test Program

The experimental program performed had two purposes. The first was to evaluate the parameter K, checking to see if its value did indeed depend primarily on M_5. The second was to compare the general form of the solutions obtained with the experimental results, once K had been established. To accomplish these goals, the experiments performed included 1) a range of Mach numbers, including both supersonic and subsonic jets; 2) a range of jet stagnation enthalpies; 3) a range of jet molecular weights; and 4) both properly and improperly expanded jets.

Table 1 High-speed runs

Gas	m_1/m_∞	$h_1{}^0/h_\infty$	γ_1	M_1	M_{eff}	u_{eff}/u_1	r_{eff}/r_1
Nitrogen	0.967	0.933	1.402	3.30	3.59	1.03	1.14
Nitrogen	0.967	0.906	1.402	3.30	2.95	0.962	0.848
Methane	0.554	1.89	1.31	[a]3.10	3.34	1.03	1.14

[a] Note that methane, flowing through the same nozzle geometry, emerges at a different M_1. This results from the different γ_1 for methane, which changes the area ratio = Mach number relationship.

High-speed tests

This first series of tests was designed to gather data on both the effects of molecular weight and the effects of over- and under-expansion at supersonic speeds. To accomplish the latter, two nitrogen jets were run through a Mach number 3.3 nozzle. However, the stagnation pressure of one was such that an underexpansion at the nozzle exit resulted ($p_1/p_\infty = 1.51$), whereas the other was such that an overexpansion existed at the exit ($p_1/p_\infty = 0.60$). The analysis assumes that the static pressure is everywhere constant and so $p_1/p_\infty = 1$; therefore, some correction must be applied. This was done by computing an effective initial Mach number, initial velocity, and exit jet radius as that which would result from an isentropic expansion (or compression) of the flow to the condition for which the static pressure in the jet is equal to the pressure in the surrounding environment. If then this effective Mach number is used as the initial condition on M_1 and the effective velocity and radius are used for the quantities u_1 and r_1, the present analysis can be applied. Part of the rationale for this transformation is that the flow, if not properly expanded initially, will eventually adjust itself to conditions that do correspond to a static pressure equal to that in the environment. These adjusted conditions will then govern the behavior of the decay, the flow having little memory of the original situation. The other part of the rationale is that the edge of a stationary inviscid jet that is not mixing with its surroundings is a free streamline of constant pressure. This pressure is equal to the ambient pressure. Thus, if a thin free-mixing layer analysis were to be applied to this inviscid picture, the proper boundary conditions would be a pressure equal to the ambient pressure throughout and a velocity difference equal to the properly expanded velocity.

To investigate the effects of the jet molecular weight at supersonic speeds, methane, a gas close to one-half the weight of nitrogen, was chosen. The same nozzle was used as in the nitrogen runs. In addition, the same degree of underexpansion as in the nitrogen run was picked to minimize any improper expansion effect if present. Thus, it was hoped that 1) the two nitrogen runs would show up the effects, if any, of improper expansion and that 2) the methane test, when compared to the underexpanded nitrogen case, would indicate any effects of molecular weight not accounted for in the analysis. A summary of the initial conditions of the three high-speed runs is given in Table 1.

The velocity decay along the axis was computed from total head pressure measurements and the data were fed into the digital computer program. Calculations of K in the developed region were obtained from several locations for each jet; the criterion for the selection of these locations was that the location was interior to at least two data points so that a good estimate of the local slope could be obtained. The results thus determined are shown by the open symbols in Fig. 2.

An evaluation of the values of K associated with the core region of each jet (K_c) was provided by the computer also. For this, Eq. (2.51) was solved for K_c using the experimentally determined core lengths X_c. The results are shown by the closed symbols in Fig. 2. It can be seen that all the values of K associated with both the core and developed regions appear to lie along a common curve, thus tending to confirm the proposition that improper expansion can be accounted for by the method described previously, which im-

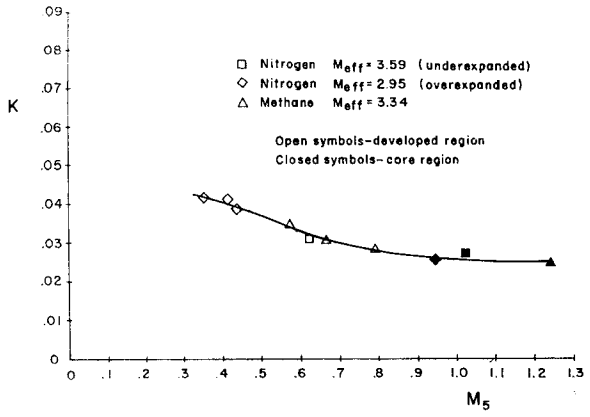

Fig. 2 High-speed test series.

plies that, so long as it does not flap, the existence of a shock structure in a free jet does not have a first-order effect upon mixing rate. Further, it appears that the effects of molecular weight enter only through their effect upon the local density so that K is only a function of the local Mach number M_5. Figure 3 shows the general character of decay curves predicted by this method together with the experimental data upon which the generation of K was based.

Low-speed tests

A series of subsonic jet mixing experiments were performed using five gases so as to provide a spread in molecular weight from 4 to 88. All gases were run at the same exit Mach number so as to eliminate, to as large a degree as possible, the effect of Mach number, and thereby isolate the effects, if any, of the wide range of molecular weights. A summary of the initial conditions of the low speed runs is given in Table 2.

Note that there was a significant spread in stagnation enthalpy. This is because of the temperature change associated with the Joule-Thompson effect in throttling from the high-pressure storage bottles to the appropriate stagnation chamber pressure, as well as the difference in c_p among the gases.

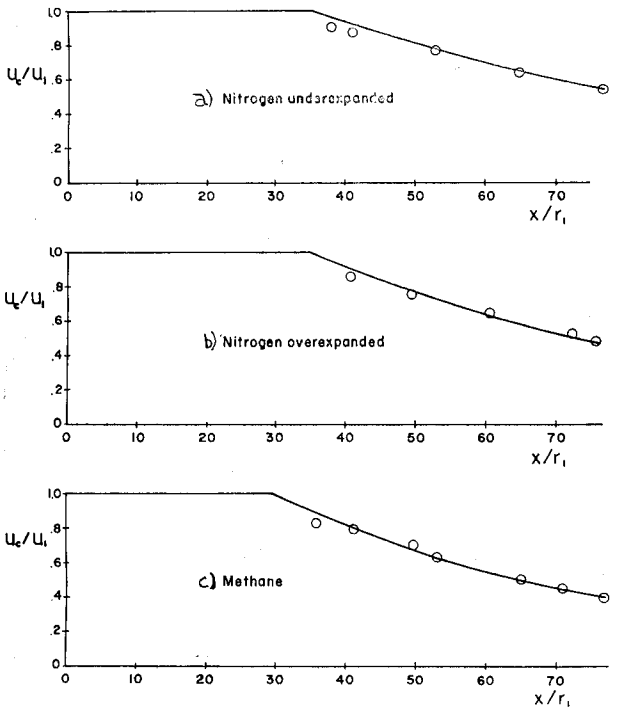

Fig. 3 Centerline velocity decays, high-speed series.

Table 2 Low-speed run series

Gas	m_1/m_∞	h_1^0/h_∞	γ_1	M_1
Helium	0.138	5.465	1.671	0.750
Methane	0.554	1.702	1.309	0.750
Nitrogen	0.967	0.871	1.402	0.750
Carbon Dioxide	1.519	0.699	1.304	0.750
Freon	3.038	0.684	1.159	0.750

Values of K for the developed regions and the cores of the five jets were initially determined in the same manner as in the high-speed tests. Despite a ratio of 22:1 in molecular weight, there appeared to be no discernible separation of the K's because of these factors. However, as a group, the values initially computed were noticeably higher than those obtained from the high-speed runs. The reason for these high values was traced to the existence of an appreciable boundary layer at the nozzle exit for the low-speed runs. Because of the relatively low velocity and the small nozzle used in these tests (exit diameter of 0.246 in.), one might expect a significant layer to be present. A survey of the jet at $M_1 = 0.75$ using air revealed an exit plane boundary-layer thickness that was 29% of the nozzle radius r_1 and a total momentum flux that was only 87.5% of the $\rho_1 u_1^2 \pi r_1^2$ assumed in the analysis [see Eq. (2.12)]. If no compensation is made in the analysis for the effects of such a layer, the more rapid decay that actually results from the lower initial momentum level and the fact that a thicker mixing layer has been built up in the jet, will be falsely attributed to higher values of K. A correction for this effect can be obtained by computing the "equivalent" jet that possesses at some station Δx_c, downstream of its origin, the same momentum flux and mass flux as does the measured jet at its exit plane. Knowing both the momentum and mass flux from profile measurements, the initial radius of the equivalent jet, r_1', and its additional core length Δx_c can be computed. When the test data then are reduced in terms of the new jet radius r_1' and a distance Δx_c is added to the measured core length, the resulting values of K then agree well with those determined from the high speed data. (This correction is discussed in more detail in Appendix C.) The values of K associated with the developed regions of each jet for the five gases tested are shown as open points in Fig. 4. Also included is the corrected value of K_c obtained as outlined above for the case of the nitrogen jet.

In Fig. 5, the low-speed and high-speed K correlations have been combined and a suggested curve has been faired through the group. Figure 6 compares the computed decay utilizing the K, M_5 faired curve of Fig. 5 with the measured decay for three of the gases.

Final Evaluation of K

Other experimental results

To gather still more data for the establishment of a K vs M_5 curve, additional experimental data were sought. One

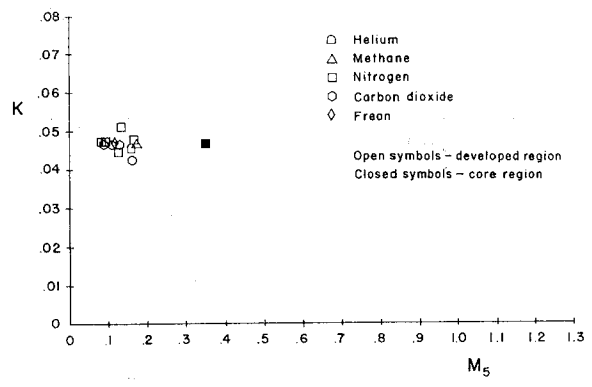

Fig. 4 Low-speed test series.

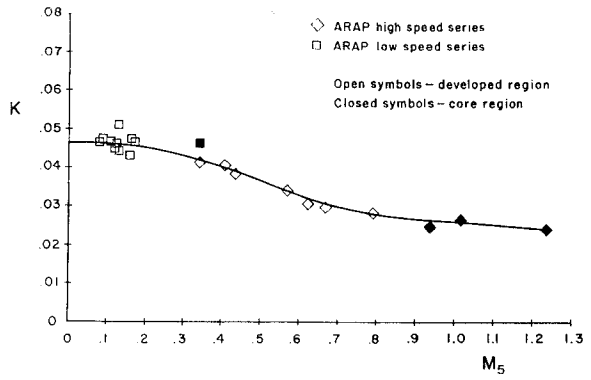

Fig. 5 Summary of tests.

obvious source was the work of Warren.[5] Although all of his experiments were performed with air mixing with air, the absence of an effect upon K of molecular weight has now been fairly well established. Submitting Warren's data to the computer, the several values of K shown in Fig. 7 were obtained.

It was noticed that these values of K were generally below the data generated at ARAP.§ A closer look at Warren's tests reveals that a sharp-edged nozzle was used. By contrast, in the ARAP test program the jet emanated from a nozzle block whose thickness was many times the exit diameter. Figure 8 indicates this contrast and also suggests the resulting difference between the two cases in the flow pattern of an entrained gas. It is reasonable to believe that a jet emanating from a flat surface will decay somewhat more rapidly than the same jet emanating from a sharp-edged nozzle because of this difference in the entrainment pattern. Indeed, a measurable drop in impingement pressure resulting from a jet in which the nozzle was surrounded by a large plate compared to the same jet in the absence of a plate has been noted in other experimental work at ARAP. More detailed measurements must be made before a definite conclusion can be reached on this point, but tentatively the curves generated from the ARAP and Warren data (Fig. 8) have been labeled blunt-edged and sharp-edged nozzle,

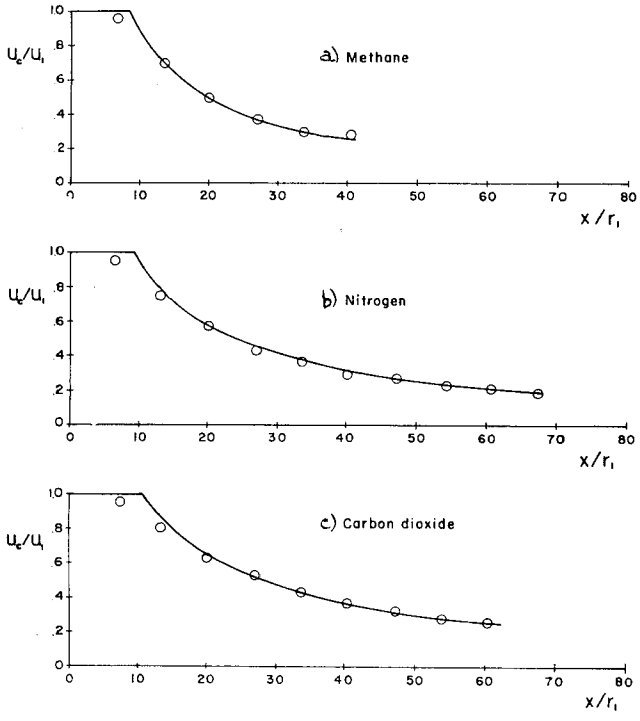

Fig. 6 Centerline velocity decays, low-speed series.

§ Warren comments on his one high K value. He feels that it may be caused by improper nozzle performance.

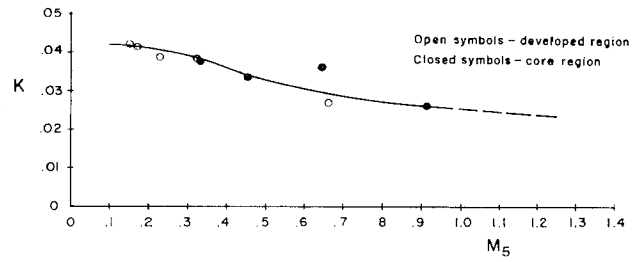

Fig. 7 Warren test series.

respectively, in the composite presentation of the K data given in Fig. 9.

In addition to Warren's tests, the incompressible work of Corrsin and Uberoi[10] and of Hinze and van der Hegge Zijnen[11] were evaluated and are also shown in Fig. 9. Remembering that a differentiation of experimental data is required to evaluate K and that such a process magnifies any scatter in the measured data, the final agreement of the K's, as shown in Fig. 9, is thought to be quite satisfactory.

A sample prediction

Attempts were made to predict the behavior of several high-enthalpy nitrogen jets measured by Avco Corporation by using the final K vs M_5 curves of Fig. 9.¶ As in the case of the ARAP low-speed tests, there was an appreciable boundary layer present as the jet emanated from a thick-edged nozzle. Utilizing the corrective procedure discussed previously for jets with boundary layer and using the values of K from the blunt-edged curve, the decay of each jet was computed and compared with the measured data. A sample of this comparison is given in Fig. 10. Note that the enthalpy ratio h_i^0/h_∞ was over 34, yet the agreement using the analysis developed in this report is excellent. It should be noted that at these high-enthalpy levels the gases are far from ideal. Nevertheless, in this case the mean c_p and m, as given by Eqs. (2.21) and (2.25), were not far different from the properly computed local, nonideal values, so that the analysis given here is applicable. This fortuitous situation cannot be expected to hold for all gases at high enthalpies. Thus, a modification of the analysis should be made to account properly for the nonideal behavior of gases if extremely high-enthalpy jets of arbitrary gases are of interest.

4. Conclusions

The results of an experimental study of compressible free jet mixing have been presented. In order to analyze these data, an extension of Warren's momentum integral method for predicting the turbulent mixing and decay of axially symmetric, compressible, free jets to the case of the mixing of dissimilar gases was developed. A comparison of the experimental results with this model of turbulent mixing permitted the following rather general conclusions to be drawn.

The decay and spreading rates of free jets appear to be local phenomena and depend, to first order, only upon the local Mach number in the vicinity of the region of maximum shear, and a correlation of the mixing-rate parameter K with the Mach number at the point where the local mean velocity has fallen to one-half its value on the jet centerline is observed.

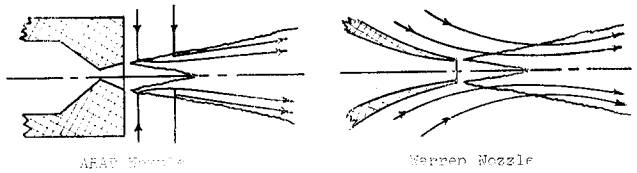

Fig. 8 Effect of nozzle configuration upon entrainment.

¶ The information of these Avco tests was made available to ARAP by R. John.[12]

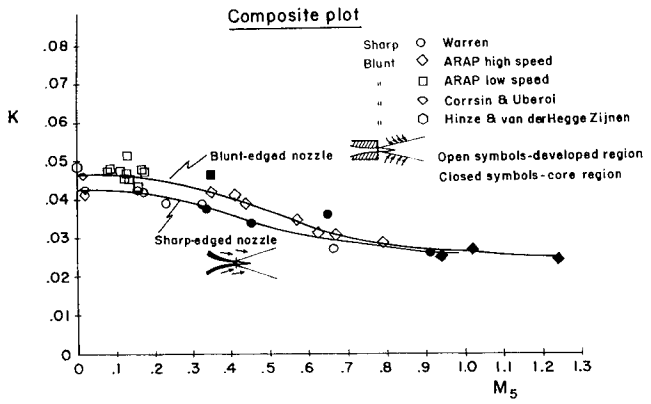

Fig. 9 Local mixing rate parameter versus local Mach number at the half-velocity radius.

The existence of a shock structure within a decaying jet does not, again to first order, affect the mixing-rate parameter K, the proper magnitude of the decay being obtained by computing the decay of the equivalent, properly expanded jet.

There appears to be an effect of the exact nozzle exit configuration on the initial decay and spreading rates. Further study of this effect is necessary, but it appears, in general, that jets issuing normally from a plane surface have, initially, a slightly higher mixing rate than those issuing from a sharp-edged nozzle.

If an appreciable amount of boundary layer exists in the nozzle that initially forms a free jet, a correction must be made to Warren's method. This correction can be obtained by computing the equivalent jet that possesses at a station Δx_c downstream of its origin, the same momentum flux and mass flux as does the measured jet at its exit plane.

Appendix A: Development of the Equations for the Core Region

In the core, the velocity profile is given by Eq. (2.13)

$$u = u_1 e^{-\lambda(r^2 - r_i^2/r_5^2 - r_i^2)} \qquad r \geq r_i$$
$$= u_1 \qquad r \leq r_i \tag{A1}$$

and the Reynolds stress by Eq. (2.16)

$$\tau_5 = K\rho_5(r_5 - r_i)(u_1/2)(\partial u/\partial r)_{r_5} \tag{A2}$$

If the same nondimensionalizations as were used previously are now introduced, i.e., $R = r/r_1$, $U = u/u_1$, $X = x/r_1$, etc., Eq. (2.30) becomes

$$\tau_5/\rho_\infty u_1^2 = (\rho_5/\rho_\infty)[\tfrac{1}{2}K_c(R_5 - R_i)](\partial U/\partial R)_{R_5} \tag{A3}$$

and Eq. (2.31) becomes

$$U = 1 \qquad \text{for} \qquad 0 \leq R \leq R_i$$
$$U = e^{-\lambda(R^2 - R_i^2/R_5^2 - R_i^2)} \qquad \text{for} \qquad R_i \leq R < \infty \tag{A4}$$

In the core, Eqs. (2.33) and (2.34) become

$$(\partial U/\partial R)_{R_5} = -\lambda R_5/(R_5^2 - R_i^2) \tag{A5}$$

and

$$RdR = -[(R_5^2 - R_i^2)dU/2\lambda U] \tag{A6}$$

When these expressions are substituted into Eqs. (2.28) and (2.29), the indicated differentiations accomplished, and the integral notation of Eqs. (2.38–2.42) adopted, one obtains two expressions analogous to Eqs. (2.43) and (2.44). (Note that integration in the core must be broken into two parts: $0 \leq R \leq R_i$, for which conditions are constant and $R_i \leq R < \infty$.)

$$I_1 - I_0 = \frac{\lambda(\rho_1/\rho_\infty)(1 - R_i^2)}{R_5^2 - R_i^2} \tag{A7}$$

$$\left[\frac{1}{2}(J_1 - J_{1/2}) - (I_1 - I_{1/2})\right]\frac{d(R_5^2 - R_i^2)}{dX} = \frac{K_c\lambda^2(\rho_5/\rho_\infty)R_5^2}{R_5 + R_i} + \frac{\lambda(\rho_1/\rho_\infty)}{2}\frac{dR_i^2}{dX} \tag{A8}$$

Equation (A7) provides R_5 as a function of R_i so that

$$R_5^2 = \frac{\lambda(\rho_1/\rho_\infty)(1 - R_i^2)}{I_1 - I_0} + R_i^2 \tag{A9}$$

and

$$\frac{d(R_5^2 - R_i^2)}{dX} = -\frac{\lambda(\rho_1/\rho_\infty)}{I_1 - I_0}\frac{dR_i^2}{dX} \tag{A10}$$

Substitution of the latter two expressions into Eq. (A8) yields

$$[f(R_i)](dR_i/dX) = K_c \tag{A11}$$

so that

$$\int_1^{R_{i*}} f(R_i)dR_i = \int_0^{X_*} K_c dX \tag{A12}$$

Although similar in form to Eq. (2.48) for the developed region (except for the change in variable from U_c to R_i), the preceding equation differs in two ways. First, as previously discussed, K_c is a constant in the core. Second, $f(R_i)$ can be integrated in closed form unlike the $f(U_c)$ in Eq. (2.48). Performing the integration yields an expression for the downstream station X as a function of core width R_i:

$$X_* = \frac{D}{K_c(\phi - 1)}\left[2 - R_{i*} - (\phi)^{1/2}(1 - \psi^2 R_{i*}^2)^{1/2} - \frac{1}{2\psi}\ln\left(\frac{1 - \psi R_{i*}}{1 + \psi R_{i*}}\cdot\frac{1 + \psi}{1 - \psi}\right)\right] \tag{A13}$$

where ψ, ϕ, and D are functions given in Appendix B. The end of the core occurs when $R_{i*} = 0$. Thus from the foregoing expression,

$$X_c = \frac{D}{K_c(\phi - 1)}\left[2 - \phi^{1/2} - \frac{1}{2\psi}\ln\left(\frac{1 + \psi}{1 - \psi}\right)\right] \tag{A14}$$

Appendix B: Complete Expressions for the Symbols Utilized in the Text

$$f(U_c) = E_c R_5 \qquad f(R_i) = DR_i(R_5 + R_i)/R_5^{2**}$$

$$D = \frac{(\rho_1/\rho_\infty)[2(I_1 - I_5) - (I_1 - I_0) - (J_1 - J_5)]}{(\rho_5/\rho_\infty)(I_1 - I_0)\lambda}$$

$$E_c = \{(I_c - I_0)[(U_c/2)(G_c - \tfrac{1}{2}G_5) - (F_c\,\tfrac{1}{2}F_5)] - F_c[\tfrac{1}{2}U_c(J_c - J_5) - (I_c - I_5)]\}[\lambda^2(\rho_5/\rho_\infty)U_c^2(I_c - I_0)]^{-1}$$

$$F = (e/V) + (fU + g/W)$$

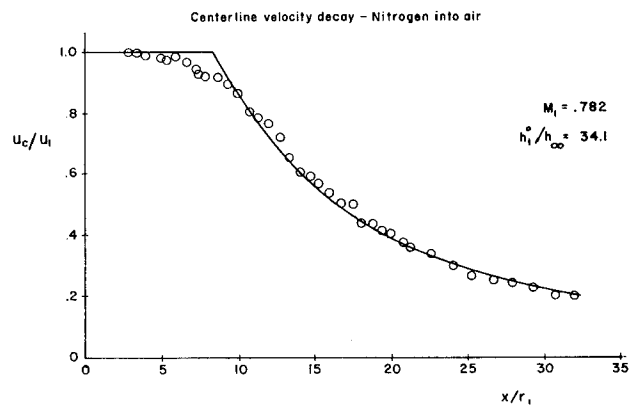

Fig. 10 Comparison of high-enthalpy test with present theory.

** Note that R^5 in the developed region is given by Eq. (2.45) and that R^5 in the core is given by Eq. (A9).

$$G = (j/V) + (kU + l/W)$$

$$I = \alpha \ln V + \beta \ln W + \gamma \ln \Phi$$

$$J = \delta \ln V + \epsilon \ln W + \zeta \ln \Phi$$

where

$$V = \mathfrak{M}U + 1 \qquad W = 1 + AU - BU^2$$

$$\Phi = (A - 2BU - q)/(A - 2BU + q)$$

$$\alpha = e/\mathfrak{M} \qquad \beta = -f/2B$$

$$\gamma = (2Bg + Af)/2Bq$$

$$\delta = j/\mathfrak{M} \qquad \epsilon = -k/2B$$

$$\zeta = (2Bl + Ak)/2Bq$$

$$e = \frac{(\mathfrak{M} - \mathcal{P})}{B + A\mathfrak{M} - \mathfrak{M}^2} \qquad f = \frac{\mathcal{P}(A - \mathfrak{M}) + B}{B + A\mathfrak{M} - \mathfrak{M}^2}$$

$$g = -e$$

$$= \frac{(\mathcal{P} - \mathfrak{M})\mathfrak{M}}{B + A\mathfrak{M} - \mathfrak{M}^2} \qquad l = \frac{B + \mathfrak{M}(A - \mathcal{P})}{B + A\mathfrak{M} - \mathfrak{M}^2}$$

$$k = \frac{(\mathcal{P} - \mathfrak{M})B}{B + A\mathfrak{M} - \mathfrak{M}^2} \qquad q = (A^2 + 4B)^{1/2}$$

$$\psi = \left(\frac{\phi - 1}{\phi}\right)^{1/2} \qquad \phi = \frac{\lambda(\rho_1/\rho_\infty)}{I_1 - I_0}$$

where A, B, $\mathfrak{M}$, and $\mathcal{P}$ are the basic run constants that describe the initial condition of the jets as discussed in the text, and the subscripts refer to evaluation of the parameters for specific values of U, i.e., 1, 0, c (for U_c), and 5 (for $U_5 = U_c/2$).

Appendix C: Boundary-Layer Correction

It was pointed out in Sec. 3 that a correction for the effect of the presence of a boundary layer at the nozzle exit plane of a jet could be obtained by the computation of an approximate equivalent jet. In this appendix, the development of this correction is given in some detail.

Referring to Fig. 11, an equivalent jet is defined as follows:

1) The momentum flux in the equivalent jet at some length Δx_c is equal to the measured momentum flux of the real jet at the nozzle exit. Thus

$$\rho_1 u_1^2 \pi r_i^2 + 2\pi \int_{r_i}^{\infty} \rho u^2 r dr = \eta[\rho_1 u_1^2 \pi r_1^2] \qquad \text{(C1)}$$

where

$$\eta \equiv \text{measured momentum flux}/\rho_1 u_1^2 \pi r_1^2$$

2) The mass flux in the equivalent jet at Δx_c is equal to the measured mass flux of the real jet at the nozzle exit. Hence,

$$\rho_1 u_1 \pi r_i^2 + 2\pi \int_{r_i}^{\infty} \rho u r dr = \eta^*[\rho_1 u_1 \pi r_1^2] \qquad \text{(C2)}$$

where

$$\eta^* \equiv \text{measured mass flux}/\rho_1 u_1 \pi r_1^2$$

Letting r_1' be the initial radius of the equivalent jet and utilizing the fact that the total momentum flux in the equivalent jet is conserved, we can also write

$$\rho_1 u_1^2 \pi r_1'^2 = \eta[\rho_1 u_1^2 \pi r_1^2] \qquad \text{(C3)}$$

or

$$(r_1'^2/r_1^2) = \eta$$

If now r_1' is used to nondimensionalize the radii in (C1) and (C2), these expressions become

$$R_i'^2 + 2\left(\frac{\rho_\infty}{\rho_1}\right) \int_{R_i'}^{\infty} \left(\frac{\rho}{\rho_\infty}\right) U^2 R' dR' = 1 \qquad \text{(C4)}$$

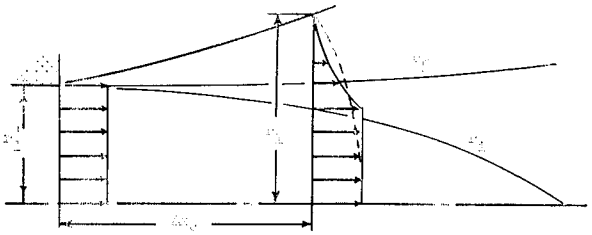

Fig. 11 Sketch showing equivalent jet nomenclature.

$$R_i'^2 + 2\left(\frac{\rho_\infty}{\rho_1}\right) \int_{R_i'}^{\infty} \left(\frac{\rho}{\rho_\infty}\right) UR' dR' = \frac{\eta^*}{\eta} \qquad \text{(C5)}$$

where the primes denote the use of r_1' for the nondimensionalization. Using Eq. (A6) from Appendix A and the I and J notation utilized previously for the resulting integrals, the preceding expressions become

$$R_i'^2 + (\rho_\infty/\rho_1)(R_5'^2 - R_i'^2)(1/\lambda)[I_1 - I_0] = 1 \qquad \text{(C6)}$$

$$R_i'^2 + (\rho/\rho_1)(R_5'^2 - R_i'^2)(1/\lambda)[J_1 - J_0] = \eta^*/\eta \qquad \text{(C7)}$$

Eliminating R_5' between these two equations yields an expression for the nondimensionalized core radius of the equivalent jet in terms of its original radius,

$$R_i'^2 = \left|\frac{(J_1 - J_0)/(I_1 - I_0) - \eta^*/\eta}{(J_1 - J_0)/(I_1 - I_0) - 1}\right| \qquad \text{(C8)}$$

Having found the core radius, the nondimensional distance back to the origin of the equivalent jet $\Delta X_c' = \Delta x_c/r_1'$ can be found from Eq. (A13) in Appendix A.

Thus, before processing the measured data from a jet with an initial boundary layer such that the initial momentum flux is $\eta[\rho_1 u_1^2 \pi r_1^2]$ and the initial mass flux is $\eta^*[\rho_1 u_1 \pi r_1^2]$, all measurements should be referred to r_1' rather than r_1 and the measured core length should, in addition, be lengthened by the amount $\Delta X_c'$ as obtained previously.

References

[1] Forstall, W., Jr. and Shapiro, A. H., "Momentum and mass transfer in coaxial gas jets," J. Appl. Mech. **17,** 399–408 (1950).

[2] Libby, P. A., "Theoretical analysis of turbulent mixing of reactive gases with application to supersonic combustion of hydrogen," J. Am. Rocket Soc. **32,** 388–396 (1962).

[3] Ferri, A., Libby, P. A., and Zakkay, V., "Theoretical and experimental investigation of supersonic combustion," *Third ACAS Congress,* Stockholm, Sweden, (August 1962); also Polytechnic Institute of Brooklyn Aerospace Lab. Rept. 713 (1962).

[4] Ferri, A., "Review of problems in application of supersonic combustion," J. Roy. Aeronaut. Soc. **68,** 575–595 (1964).

[5] Warren, W. R., "An analytical and experimental study of compressible free jets," Princeton Univ. Dept. of Aeronautical Engineering, Rept. 381 (1957).

[6] Ferri, A., "Axially symmetric heterogeneous mixing," International Union of Theoretical and Applied Mechanics, International Symposium on Applications of the Theory of Functions in Continuum Mechanics, Tbilisi, Russia (September 1963); also Polytechnic Institute of Brooklyn, Aerospace Labs., Rept. 787 (1963).

[7] Zakkay, V., Krause, E., and Woo, S. D., "Turbulent transport properties for axisymmetric heterogeneous mixing," AIAA J. **2,** 1939–1947 (1964).

[8] Reichardt, H., "Gesetzmäbigkeiten der freien Turbulenz," VDI-Forschungsheft **414** (1942), 2nd ed. (1951).

[9] Zimm, W., "Uber die Strömungsvorgänge im freien Luftstrahl," VDI-Forschungsheft **234** (1921).

[10] Corrsin, S. and Uberoi, M. S., "Further experiments on the flow and heat transfer in a heated turbulent air jet," NACA TM 1865 (1949); also available as NACA Rept. 998 (1950).

[11] Hinze, J. O. and van der Hegge Zijnen, B. G., "Transfer of heat and matter in the turbulent mixing zone of an axially symmetric jet," *Proceedings of the 7th Inter'l Congress for Applied Mechanics* (London, 1948), Vol. 2, p. 286.

[12] John, R., private communication.